

Heat capacities and thermodynamic properties of MgBTC

Li-Fang Song · Chun-Hong Jiang · Jian Zhang ·
Li-Xian Sun · Fen Xu · Yun-Qi Tian · Wan-Sheng You ·
Zhong Cao · Ling Zhang · Dao-Wu Yang

Received: 11 June 2009 / Accepted: 22 July 2009 / Published online: 28 August 2009
© Akadémiai Kiadó, Budapest, Hungary 2009

Abstract A novel two-dimensional metal organic framework MgBTC [MgBTC(OCN)₂·2H₂O, where BTC = 1,3,5-benzenetricarboxylate] has been synthesized solvothermally and characterized by single crystal XRD, powder XRD, FT-IR spectra. The low-temperature molar heat capacities of MgBTC were measured by temperature modulated differential scanning calorimetry (TMDSC) over the temperature range from 190 to 350 K for the first time. No phase transition or thermal anomaly was observed in the experimental temperature range. The thermodynamic parameters of MgBTC such as entropy and enthalpy relative to reference temperature of 298.15 K were derived based on the above molar heat capacities data. Moreover, the thermal stability and decomposition of MgBTC was further investigated through thermogravimetry (TG)-mass spectrometer (MS). Four stages of mass loss were observed in the TG curve. TG-MS curve indicated that the products of oxidative degradation of MgBTC are H₂O, N₂, CO₂ and CO.

The powder XRD showed that the mixture after TG contains MgO and graphite.

Keywords Magnesium · MDSC · Metal organic frameworks · Molar heat capacity · TG

Introduction

Metal-organic frameworks (MOFs) have attracted a great deal of interests recently because of its potential application in gas storage [1], ion exchange [2], catalysis [3], chemical sensor [4, 5], and separation [6]. This series of materials are generally constructed by transitional metal ions and polyfunctional organic linkers. However, alkali metals [5, 7, 8] or alkaline-earth metals [9] constructed MOFs are rarely investigated. Actually, these light metals have the priority in building frameworks with light volumetric density and novel topology.

Molar heat capacities of the materials at different temperatures are basic data in chemistry and engineering, from which many other thermodynamic properties such as enthalpy and entropy can be calculated. These parameters are important for both theoretical and practical purposes. Heat capacities determinations of various compounds have attracted many researchers' attention.

It is generally accepted that heat capacity is one of the most fundamental thermodynamic properties of substances and that it is closely related to other physical and chemical properties. Heat capacity determinations of various compounds have been focused by many researchers. Modulated differential scanning calorimetry (MDSC) is one of the easier and more accurate methods for determining the heat capacity. In 1992, MDSC was initially proposed by Reading and co-workers [10], who applied a small sinusoidal

L.-F. Song · C.-H. Jiang · J. Zhang · L.-X. Sun (✉)
Materials and Thermochemistry Laboratory, Dalian Institute
of Chemical Physics, Chinese Academy of Sciences, 457,
Zhongshan Road, 116023 Dalian, Peoples Republic of China
e-mail: lxsun@dicp.ac.cn

F. Xu (✉) · Y.-Q. Tian · W.-S. You
Faculty of Chemistry and Chemical Engineering, Liaoning
Normal University, 116029 Dalian, Peoples Republic of China
e-mail: xufen@lnnu.edu.cn; fenxu@dicp.ac.cn

L.-F. Song · C.-H. Jiang
Graduate School of the Chinese Academy of Sciences, 100049
Beijing, Peoples Republic of China

Z. Cao · L. Zhang · D.-W. Yang
School of Chemistry and Biological Engineering, Changsha
University of Science and Technology, 410076 Changsha,
Peoples Republic of China

modulation of temperature superimposed onto a linear underlying heating rate as an extension of the conventional DSC. The structure and principle of the calorimeter have been described in detail by the literatures [11–13]. Recently, this method has been greatly developed for directly determining heat capacities for various materials isothermally and non-isothermally [14–16].

In the present paper, we reported one novel alkaline-earth MOFs named MgBTC, the low-temperature molar heat capacity of which was measured by TMDSC and the thermodynamic parameters such as entropy and enthalpy were also calculated. The accuracy of TMDSC was established by comparing the measured heat capacities of standard sapphire (α - Al_2O_3) with previously reported values (NIST and NBS) [17, 18]. The thermal decomposition characteristics of the compound was investigated by TG-MS.

Experimental

Sample

MgBTC has been synthesized by solvothermally reaction. All chemicals and reagents were commercially available of analytical grade and were used as received. A mixture of $\text{Mg}(\text{NO}_3)_2 \cdot 6\text{H}_2\text{O}$ (0.20 g, 0.78 mmol), H_3BTC (0.10 g, 0.48 mmol) and DMF (15 mL) was sealed in a 40 mL Teflon-lined stainless steel autoclave and heated at 403 K for 24 h, then cooled to room temperature naturally. After filtration, the product was washed with DMF and then dried at 323 K in vacuum overnight. Colorless block crystals suitable for single crystal X-ray diffraction analysis were obtained in ca. 82% yield based on Mg(II).

Characterization

The crystal data were collected at 293 K using a SMART APEX II-CCD single crystal XRD (graphite monochromated Mo $K\alpha$ radiation, $\lambda = 0.71073 \text{ \AA}$). A multi-scan absorption correction was applied using the SADABS program. The structures were solved by direct method and refined by full-matrix least-squares method implemented in SHELXTL-97 [19]. All the non-hydrogen atoms were refined anisotropically. Hydrogen atoms were added theoretically. The program Mercury 1.4.2 was used for calculation of X-ray crystallographic powder patterns of MgBTC. FT-IR spectra were recorded on a Nicolet 380 FT-IR spectrometer using KBr pellet in the wavelength range of 4,000–400 cm^{-1} . Powder XRD experiments were carried out on a PANalytical X-ray Diffractometer (X'Pert MPD PRO, Cu $K\alpha$, 40 kV, 40 mA).

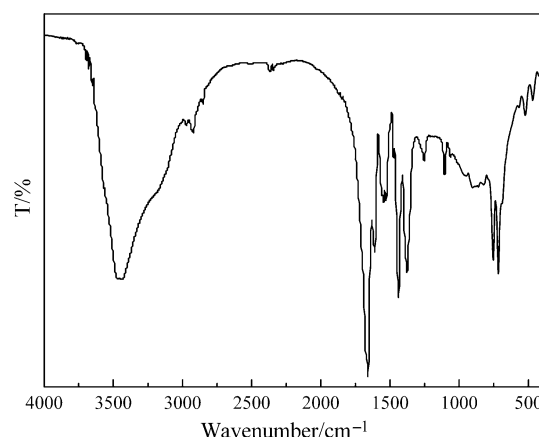


Fig. 1 IR spectra of MgBTC

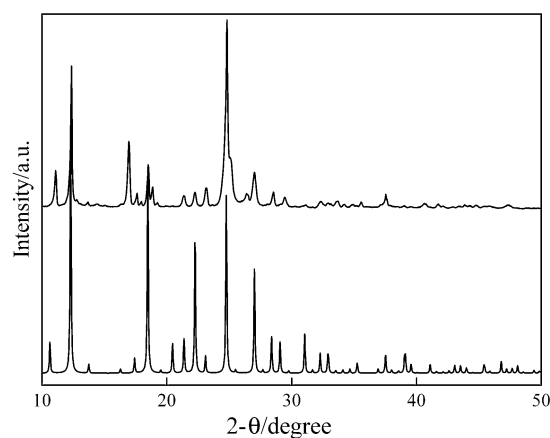


Fig. 2 Experimental and simulated powder XRD pattern of MgBTC

Crystal data for the complex are as follows: hexagonal system, $P6_3/m$ (no. 176), $a = 16.6217(5)$, $b = 16.6217(5)$, $c = 14.366(3)$, $\alpha = 90^\circ$, $\beta = 90^\circ$, $\gamma = 120^\circ$. CCDC number: 704531. The molar mass of MgBTC is 351.50. The FT-IR spectra are shown in Fig. 1. The purity of MgBTC was determined by the powder XRD. The resolved diffraction peaks match the crystal data sample perfectly, and no characteristic peaks of impurities were observed (Fig. 2). Before thermal experiments, the sample was heated at 323 K in vacuum for 6 h.

Heat capacity measurement

Heat capacity measurements of the MgBTC were performed on DSC Q1000 (T-zero DSC-technology, TA Instruments Inc., USA). A mechanical cooling system was used for the experimental measurement. Dry nitrogen gas with high purity (99.999%) was used as purge gas (50 mL min^{-1}) through the DSC cell. The temperature scale of the instrument was initially calibrated in the

standard DSC mode, using the extrapolated onset temperatures of the melting of indium (429.75 K) at a heating rate of 10 K min⁻¹. The energy scale was calibrated with the heat of fusion of indium (28.45 J g⁻¹). The heat capacity calibration was made by running a standard sapphire (α -Al₂O₃) at the experimental temperature. The calibration method and the experiment were performed at the same conditions as follows: (1) sampling interval: 1.00 s/pt; (2) zero heat flow at 253.15 K; (3) equilibrate at 133.15 K; (4) modulate temperature amplitude of ± 0.5 K with period of 100 s; (5) isothermal for 5.00 min; (6) temperature ramp at 5 K min⁻¹ to 413 K. The constants of heat capacity for the MDSC: $K_{\text{total}} = 1.024$; $K_{\text{reversible}} = 1.019$.

The masses of the reference and sample pans with lids were within 30 ± 0.05 mg. Samples were crimped in non-hermetic aluminum pans with lids. Sample mass was weighed on a METTLER TOLEDO electrobalance (AB135-S, Classic) with an accuracy of (± 0.01 mg).

Thermal analysis

Thermogravimetric analysis (TG) was carried out on Cahn Thermax 500 from 300 to 1,173 K. The heating rate was 10 K min⁻¹ and the flow rate of argon (99.999%) was 100 mL min⁻¹. The TG equipment was calibrated by the CaC₂O₄·H₂O (99.9%). The mass of MgBTC was 42.92 mg. Mass spectra (MS) were performed on a Multicomponent Online Gas Analyzer GAM 200.

Results and discussion

Heat capacity of standard sapphire (α -Al₂O₃)

Heat capacity measurement of each compound is repeated three times under the same condition unless stated elsewhere. The emphasis of this work is to assess the reproducibility and ensure accuracy of the measured data using TMDSC (Q1000). For standard sapphire measurement, the data of three reduplicate experiments and the experimental standard deviation were given in our previous work [16]. The experimental standard deviation is during ± 0.0044 , which shows that the testing system of TMDSC is steady. Relative deviations have been calculated by the following equation:

$$\text{RD}(\%) = 10^2 [C_{p,m}(\text{exp}) - C_{p,m}(\text{ref})] / C_{p,m}(\text{ref}) \quad (1)$$

where $C_{p,m}(\text{exp})$ is the experimental heat capacities and $C_{p,m}(\text{ref})$ is the referenced heat capacities. The results show that the relative deviation of our calibration data from the recommended value [17] over the whole temperature range was within $\pm 1.5\%$.

Heat capacities of MgBTC

The data of three reduplicate experiments and the experimental standard deviation for MgBTC are given in Table 1. The experimental standard deviations below 0.16 are obtained and show reasonably good reproducibility in the temperature range from 190 to 350 K. The experimental molar heat capacities curve of MgBTC versus temperature is shown in Fig. 3. The experimental and fitted data are listed in Table 2.

The molar heat capacities of the sample are fitted to the following polynomial equation of heat capacities ($C_{p,m}$)

Table 1 The data of three reduplicate experiments for MgBTC

T/ K	$C_{p,m}(\text{exp})/\text{J K}^{-1} \text{g}^{-1}$				Standard deviation
	<i>a</i>	<i>b</i>	<i>c</i>	Average	
190	0.9780	0.9678	0.9885	0.9781	0.010
195	0.9940	0.9835	1.0060	0.9945	0.011
200	1.0090	0.9983	1.0200	1.0091	0.011
205	1.0260	1.0160	1.0370	1.0263	0.011
210	1.0440	1.0360	1.0570	1.0457	0.011
215	1.0610	1.0550	1.0770	1.0643	0.011
220	1.0780	1.0740	1.0960	1.0827	0.012
225	1.0970	1.0910	1.1140	1.1007	0.012
230	1.1150	1.1100	1.1320	1.1190	0.012
235	1.1320	1.1280	1.1500	1.1367	0.012
240	1.1510	1.1480	1.1690	1.1560	0.011
245	1.1680	1.1680	1.1880	1.1747	0.012
250	1.1870	1.1880	1.2080	1.1943	0.012
255	1.2060	1.2070	1.2250	1.2127	0.011
260	1.2300	1.2330	1.2510	1.2380	0.011
265	1.2520	1.2580	1.2750	1.2617	0.012
270	1.2760	1.2850	1.3030	1.2880	0.014
275	1.3030	1.3160	1.3340	1.3177	0.016
280	1.3360	1.3490	1.3680	1.3510	0.016
285	1.3480	1.3810	1.3940	1.3743	0.024
290	1.3610	1.3790	1.4020	1.3807	0.021
295	1.3850	1.4010	1.4280	1.4047	0.022
300	1.4080	1.4350	1.4650	1.4360	0.029
305	1.4390	1.4810	1.5150	1.4783	0.038
310	1.4800	1.5420	1.5790	1.5337	0.05
315	1.5320	1.6140	1.6560	1.6007	0.063
320	1.5940	1.6980	1.7470	1.6797	0.078
325	1.6640	1.7990	1.8500	1.7710	0.096
330	1.7360	1.9040	1.9520	1.8640	0.11
335	1.8040	2.0120	2.0530	1.9563	0.13
340	1.8600	2.1030	2.1270	2.0300	0.15
345	1.9060	2.1800	2.1800	2.0887	0.16
350	1.9450	2.1960	2.1710	2.1040	0.14

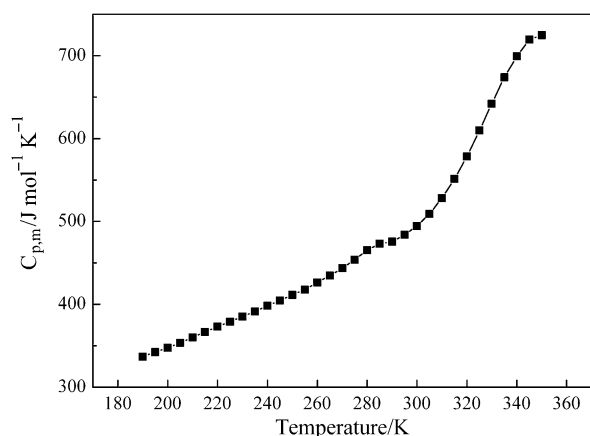


Fig. 3 Molar heat capacities ($C_{p,m}$) of MgBTC as a function of temperature

with reduced temperature (X) using the OriginPro 7.5 software:

From 190 to 280 K,

$$C_{p,m}(\text{JK}^{-1}\text{mol}^{-1}) = 399.7 + 58.33X + 2.477X^2 + 7.282X^3 + 7.241X^4 \quad (2)$$

where $X = (T - 235)/45$, and T is the experimental temperature, 235 is obtained from polynomial $(T_{\max} + T_{\min})/2$, 45 is obtained from polynomial $(T_{\max} - T_{\min})/2$, T_{\max} is the upper limit (280 K) of the above temperature region, T_{\min} is the lower limit (190 K) of the above temperature region. The correlation coefficient is $R^2 = 0.99995$. The

relative deviations of all the experimental points from the fitting heat capacities values are within $\pm 0.18\%$.

From 280 to 350 K,

$$C_{p,m}(\text{JK}^{-1}\text{mol}^{-1}) = 562.7 + 186.3X + 104.9X^2 - 53.81X^3 - 59.99X^4 \quad (3)$$

where $X = (T - 315)/35$, and T is the experimental temperature, 315 is obtained from polynomial $(T_{\max} + T_{\min})/2$, 35 is obtained from polynomial $(T_{\max} - T_{\min})/2$, T_{\max} is the upper limit (350 K) of the above temperature region, T_{\min} is the lower limit (280 K) of the above temperature region. Correlation coefficient R^2 is 0.99992. The relative deviations of all the experimental points from the fitting heat capacities values are within $\pm 0.38\%$.

From Fig. 3, it can be seen that the heat capacity of the sample increases with increasing temperature in a smooth and continuous manner in the experimental temperature range. The curve indicates two thermal anomalies at 280 and 340 K. The small anomaly around 280 K is due to the change of H_2O in the framework. The anomaly around 340 K is because of the decomposition of the sample, and TG curve indicated the mass loss started at 340 K. In the whole temperature range, no obvious phase transition can be observed, which indicates that this sample is stable in the experimental temperature range.

Thermodynamic functions of MgBTC

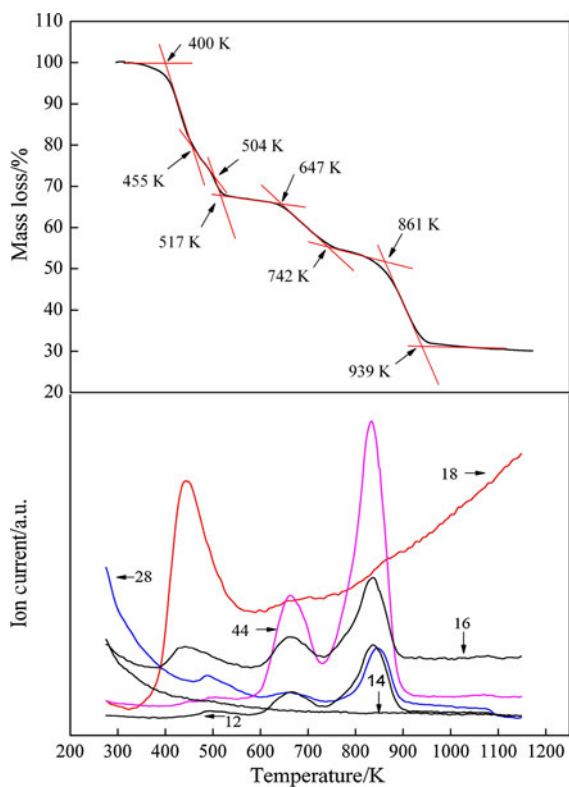
Enthalpy and entropy of substances are basic thermodynamic functions. In terms of the polynomials of molar heat

Table 2 The experimental and fitted molar heat capacities of MgBTC

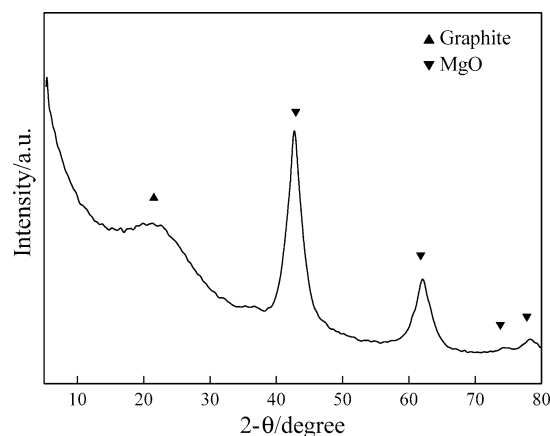
T/K	$C_{p,m}(\text{exp})/\text{J K}^{-1}\text{mol}^{-1}$	$C_{p,m}(\text{fit})/\text{J K}^{-1}\text{mol}^{-1}$	RD/%	T/K	$C_{p,m}(\text{exp})/\text{J K}^{-1}\text{mol}^{-1}$	$C_{p,m}(\text{fit})/\text{J K}^{-1}\text{mol}^{-1}$	RD/%
190	343.8	343.8	0.0011	275	463.2	463.1	-0.0041
195	349.6	349.2	-0.10	280	474.9	475.0	0.032
200	354.7	355.1	0.10	285	483.1	481.6	-0.31
205	360.8	361.2	0.12	290	485.3	487.1	0.38
210	367.6	367.5	-0.014	295	493.7	494.1	0.081
215	374.1	373.9	-0.055	300	504.8	504.3	-0.083
220	380.6	380.4	-0.054	305	519.6	518.9	-0.14
225	386.9	386.8	-0.022	310	539.1	538.4	-0.13
230	393.3	393.2	-0.022	315	562.6	562.7	0.012
235	399.5	399.7	0.041	320	590.4	591.3	0.15
240	406.3	406.2	-0.027	325	622.5	622.8	0.053
245	412.9	412.9	-0.0032	330	655.2	655.6	0.054
250	419.8	419.8	-0.0073	335	687.7	687.0	-0.099
255	426.3	427.0	0.18	340	713.5	714.1	0.073
260	435.2	434.8	-0.080	345	734.2	733.2	-0.13
265	443.5	443.3	-0.045	350	739.6	740.1	0.074
270	452.7	452.6	-0.020				

Table 3 Calculated thermodynamic function data of MgBTC

T/K	$H_T - H_{298.15}/$ kJ mol^{-1}	$S_T - S_{298.15}/$ $\text{J K}^{-1} \text{mol}^{-1}$	T/K	$H_T - H_{298.15}/$ kJ mol^{-1}	$S_T - S_{298.15}/$ $\text{J K}^{-1} \text{mol}^{-1}$
190	-47.53	-184.9	275	-13.70	-39.01
195	-45.80	-175.9	280	-11.36	-30.56
200	-44.04	-167.0	285	-8.282	-22.10
205	-42.25	-158.1	290	-5.169	-13.67
210	-40.43	-149.3	295	-2.016	-5.278
215	-38.58	-140.6	298.15	0	0
220	-36.69	-132.0	300	1.191	3.105
225	-34.77	-123.3	305	4.478	11.55
230	-32.82	-114.8	310	7.873	20.13
235	-30.84	-106.2	315	11.41	28.93
240	-28.83	-97.75	320	15.12	38.01
245	-26.78	-89.30	325	19.02	47.43
250	-24.70	-80.89	330	23.13	57.19
255	-22.58	-72.51	335	27.44	67.29
260	-20.42	-64.15	340	31.95	77.67
265	-18.23	-55.78	345	36.61	88.24
270	-15.99	-47.41	350	41.35	98.86

**Fig. 4** TG-MS curves of MgBTC

capacity and the thermodynamic relationship, the $[H_T - H_{298.15}]$ and $[S_T - S_{298.15}]$ of MgBTC was calculated in the temperature ranges from 190 to 350 K with an interval of 5 K relative to the temperature of 298.15 K. The thermodynamic relationships are as follows:

**Fig. 5** Powder XRD pattern of MgBTC after TGA

$$H_T - H_{298.15} = \int_{298.15}^T C_{p,m} dT \quad (4)$$

$$S_T - S_{298.15} = \int_{298.15}^T (C_{p,m}/T) dT \quad (5)$$

The calculated thermodynamic functions $[H_T - H_{298.15}]$ and $[S_T - S_{298.15}]$ are shown in Table 3.

Thermal stabilities and decomposition of MgBTC

TG analysis (Fig. 4) shows that a four-stage mass loss occurs in the temperature range of 300–1,173 K. The mass loss of the first two stages is about 32.20% (calculated

34.16%) in the temperature range of 373–517 K, it is due to dehydrate from MgBTC(OCN)₂·2H₂O to MgBTC. The decomposed products are H₂O (*m/z* = 16, 18), CO (*m/z* = 12, 28), N₂ (*m/z* = 14, 28) and CO₂ (*m/z* = 12, 44), which was validated by MS (Fig. 4). Further decomposition of MgBTC of the last two stages occurs in the region of 517–939 K. The decomposed products of this temperature range are mainly H₂O (*m/z* = 16, 18), CO (*m/z* = 12, 28) and CO₂ (*m/z* = 12, 44) as shown in TG-MS curve, and the mass loss is 36.53% according to the incomplete degradation of the benzenetricarboxylate ligands, powder XRD (Fig. 5) was carried out to validate that MgBTC was decomposed to MgO and graphite till the end of the temperature.

Conclusions

In this work, MgBTC has been synthesized solvothermally and characterized by single crystal X-ray diffraction, powder XRD, FT-IR spectra. The molar heat capacities of MgBTC were measured from 190 to 350 K using TMDSC for the first time. The thermodynamic function data relative to the reference temperature (298.15 K) were calculated based on the heat capacities measurements. Moreover, the thermal stability of MgBTC was further investigated by TG-MS.

Acknowledgements The authors gratefully acknowledge the financial support for this work from the National Natural Science Foundation of China (No. 2083309, 20873148, 50671098 and U0734005), the National High Technology Research and Development Program (863 Program) of China (No. 2007AA05Z115 and 259 2007AA05Z102), the National Basic Research Program (973 program) of China (2010CB631303) and IUPAC (No. 2008-006-3-100).

References

- Dinca M, Long JR. Hydrogen storage in microporous metal-organic frameworks with exposed metal sites. *Angew Chem Int Ed.* 2008;47:6766–79.
- Lu WG, Su CY, Lu TB, Jiang L, Chen JM. Two stable 3D metal-organic frameworks constructed by nanoscale cages via sharing the single-layer walls. *J Am Chem Soc.* 2006;128:34–5.
- Xamena FXLI, Abad A, Corma A, Garcia H. MOFs as catalysts: activity, reusability and shape-selectivity of a Pd-containing MOF. *J Catal.* 2007;250:294–8.
- Winter S, Weber E, Eriksson L, Csoregh I. New coordination polymer networks based on copper(II) hexafluoroacetylacetonate and pyridine containing building blocks: synthesis and structural study. *New J Chem.* 2006;30:1808–19.
- Liu YY, Zhang J, Xu F, Sun LX, Zhang T, You WS, et al. Lithium-based 3D coordination polymer with hydrophilic structure for sensing of solvent molecules. *Cryst Growth Des.* 2008;8:3127–9.
- Bae YS, Mulfort KL, Frost H, Ryan P, Punnathanam S, Broadbelt LJ, et al. Separation of CO₂ from CH₄ using mixed-ligand metal-organic frameworks. *Langmuir.* 2008;24:8592–8.
- Ferey G, Millange F, Morcrette M, Serre C, Doublet ML, Greneche JM, et al. Mixed-valence Li/Fe-based metal-organic frameworks with both reversible redox and sorption properties. *Angew Chem Int Ed.* 2007;46:3259–63.
- Liu YY, Zhang H, Sun LX, Xu F, You WS, Zhao Y. Solvothermal synthesis and characterization of a lithium coordination polymer possessing a highly stable 3D network structure. *Inorg Chem Commun.* 2008;11:396–9.
- Williams CA, Blake AJ, Wilson C, Hubberstey P, Schroeder M. Novel metal-organic frameworks derived from group II metal cations and aryldicarboxylate anionic ligands. *Cryst Growth Des.* 2008;8:911–22.
- Reading M, Elliott D, Hill V. Some aspects of the theory and practise of modulated differential scanning calorimetry. In: *Proceedings of the 21st North American Thermal Analysis Society Conference, Atlanta, Georgia.* 1992. pp. 145–50.
- Wunderlich B, Jin YM, Boller A. Mathematical-description of differential scanning calorimetry based on periodic temperature modulation. *Thermochim Acta.* 1994;238:277–93.
- Danley RL. New modulated DSC measurement technique. *Thermochim Acta.* 2003;402:91–8.
- Wunderlich B. The contributions of MDSC to the understanding of the thermodynamics of polymers. *J Therm Anal Calorim.* 2006;85:179–87.
- Chau J, Garlicka I, Wolf C, Teh J. Modulated DSC as a tool for polyethylene structure characterization. *J Therm Anal Calorim.* 2007;90:713–9.
- Qi YN, Xu F, Ma HJ, Sun LX, Zhang J, Jiang T. Thermal stability and glass transition behavior of PANI/gamma-Al₂O₃ composites. *J Therm Anal Calorim.* 2008;91:219–23.
- Qiu SJ, Chu HL, Zhang J, Qi YN, Sun LX, Xu F. Heat capacities and thermodynamic properties of CoPc and CoTMPP. *J Therm Anal Calorim.* 2008;91:841–8.
- Archer DG. Thermodynamic properties of synthetic sapphire (Alpha-Al₂O₃), standard reference material 720 and the effect of temperature-scale differences on thermodynamic properties. *J Phys Chem Ref Data.* 1993;22:1441–53.
- Ginnings DC, Furukawa GT. Heat capacity standards for the range 14-degrees-K to 1200-degrees-K. *J Am Chem Soc.* 1953;75:522–7.
- Sheldrick GM. SHELX97, program for crystal structure refinement. Germany: Göttingen University; 1997.